

Published in final edited form as:

*Oncogene*. 2013 September 26; 32(39): . doi:10.1038/onc.2012.501.

## Transcriptional Intermediary Factor 1 $\gamma$ binds to the Anaphase-Promoting Complex/Cyclosome and promotes mitosis

Garry G. Sedgwick<sup>\*†</sup>, Kelly Townsend<sup>\*</sup>, Ashley Martin<sup>\*</sup>, Neil J. Shimwell<sup>\*</sup>, Roger J. A. Grand<sup>\*</sup>, Grant S. Stewart<sup>\*</sup>, Jakob Nilsson<sup>†</sup>, and Andrew S. Turnell<sup>\*‡</sup>

<sup>\*</sup>School of Cancer Sciences, College of Medical and Dental Sciences, The University of Birmingham, Edgbaston, Birmingham B15 2TT, UK

<sup>†</sup>NNF Center for Protein Research, The University of Copenhagen, Blegdamsvej 3b, DK-2200, Copenhagen N, Denmark

### Abstract

The Anaphase-Promoting Complex/Cyclosome (APC/C) is an ubiquitin ligase that functions during mitosis. Here we identify the transcriptional regulator, Transcriptional Intermediary Factor 1 $\gamma$ , TIF1 $\gamma$  as an APC/C-interacting protein that regulates APC/C function. TIF1 $\gamma$  is not a substrate for APC/C-dependent ubiquitylation but instead, associates specifically with the APC/C holoenzyme and Cdc20 to affect APC/C activity and progression through mitosis. RNA interference studies indicate that TIF1 $\gamma$  knockdown results in a specific reduction in APC/C ubiquitin ligase activity, the stabilization of APC/C substrates, and an increase in the time taken for cells to progress through mitosis from nuclear envelope breakdown (NEBD) to anaphase. TIF1 $\gamma$  knockdown cells are also characterized by the inappropriate presence of cyclin A at metaphase, and an increase in the number of cells that fail to undergo metaphase-to-anaphase transition. Expression of a siRNA-resistant TIF1 $\gamma$  species relieves the mitotic phenotype imposed by TIF1 $\gamma$  knockdown and allows for mitotic progression. Binding studies indicate that TIF1 $\gamma$  is also a component of the APC/C-Mitotic Checkpoint Complex (MCC), but is not required for MCC dissociation from the APC/C once the Spindle Assembly Checkpoint (SAC) is satisfied. TIF1 $\gamma$  inactivation also results in chromosome misalignment at metaphase, and SAC activation; inactivation of the SAC relieves the mitotic block imposed by TIF1 $\gamma$  knockdown. Together these data define novel functions for TIF1 $\gamma$  during mitosis and suggest that a reduction in APC/C ubiquitin ligase activity promotes SAC activation.

### INTRODUCTION

The APC/C is a multiprotein E3 ubiquitin ligase complex that coordinates mitotic progression and exit through targeting substrates such as Securin and cyclin B1 for proteasomal-mediated degradation (1, 2). APC/C activity is controlled by the cell cycle-dependent recruitment of one of two activators, Cdc20 or Cdh1, to specific APC/C proteins (1, 2). Cdc20 and Cdh1 also serve in conjunction with particular APC/C subunits to bind substrates (1, 2). APC/C-Cdc20 regulates metaphase-to-anaphase transition primarily by targeting the Separase inhibitor, Securin, for degradation (1). APC/C-Cdc20 activity is tightly controlled by the SAC which monitors microtubule attachment to kinetochores, and ensures the fidelity of sister chromatid segregation at anaphase (2, 3). When the SAC is

<sup>‡</sup>To whom correspondence should be addressed: a.s.turnell@bham.ac.uk.

*Author contributions:* AST initiated the study; GGS, JN and AST designed the study; GGS, KT, AM, NJS, JN and AST performed experiments and analyzed data. RJAG and GSS helped supervise the study. AST wrote the paper.

The authors declare they have no conflict of interest.

activated by the presence of unattached kinetochores, SAC components MAD2, BubR1 and Bub3 all serve to inhibit APC/C-Cdc20 activity, and metaphase-to-anaphase transition (2, 3). APC/C-Cdc20 and APC/C-Cdh1 are also regulated by the transcriptional co-activators CBP and p300, which bind to APC/C subunits APC5 and APC7, through interaction domains conserved in adenovirus E1A (4, 5). The DNA damage response protein, MDC1 also regulates APC/C-Cdc20 activity during mitosis and functions independently of SAC and DNA damage response pathways, to facilitate Cdc20 association with the APC/C (6).

TIF1 $\gamma$  also known as TRIM33 and hEctodermin is a member of the Tripartite Motif/RING finger, B-boxes, and a coiled coil domain (TRIM/RBCC) family of proteins (7). It was initially identified as a transcriptional repressor and along with TIF1 $\alpha$  has been shown to be fused to the RET receptor tyrosine kinase in childhood papillary thyroid carcinomas (8, 9). The zebra fish TIF1 $\gamma$  ortholog, *mon*, is required for differentiation of erythroid progenitor cells and posterior mesenchymal cells (10). Recent work suggests that the TGF- $\beta$  dependent differentiation of hematopoietic, mesenchymal, and epithelial cells is dependent upon the ability of TIF1 $\gamma$  to compete with SMAD4 for binding to activated SMAD2/SMAD3 transcription factor complexes (11). Other workers suggest that TIF1 $\gamma$  serves as a SMAD4 monoubiquitin ligase and inhibits TGF- $\beta$  signalling pathways by dissociating SMAD2/3-SMAD4 complexes (12, 13).

To explore further the complexity of APC/C function we undertook mass spectrometric analyses to identify novel APC/C-binding partners. Here, we detail the characterization of TIF1 $\gamma$  as an APC/C-interacting protein that affects APC/C activity in mitosis. We show that TIF1 $\gamma$  interacts specifically with APC3 and Cdc20, and regulates cell cycle progression through mitosis; TIF1 $\gamma$  knockdown reduces APC/C-Cdc20 ligase activity, stabilizes APC/C substrate levels and leads to an accumulation of cells in metaphase. Consistent with these observations, the time taken for cells to pass from NEBD to anaphase increases significantly following TIF1 $\gamma$  knockdown. Indeed, a significant proportion of TIF1 $\gamma$  knockdown cells fail to undergo metaphase-to-anaphase transition. TIF1 $\gamma$  knockdown cells are also characterized by the inappropriate expression of APC/C substrate cyclin A at metaphase and metaphases with misaligned chromosomes. Consistent with a role for TIF1 $\gamma$  in mitosis, a small interfering (si)RNA-resistant TIF1 $\gamma$  relieves the mitotic block imposed by TIF1 $\gamma$  knockdown and allows for cell cycle progression. The mitotic phenotype exhibited by TIF1 $\gamma$  knockdown cells is also relieved by inactivation of the SAC, suggesting that TIF1 $\gamma$  activity in mitosis is monitored by the SAC, such that TIF1 $\gamma$  inactivation results in SAC activation. Taken together, this work defines a new role for TIF1 $\gamma$  in regulating progression through mitosis.

## RESULTS

### TIF1 $\gamma$ associates with the APC/C and Cdc20 but it is not a substrate for APC/C-directed ubiquitylation

In order to identify novel APC/C-interacting proteins we performed immunoprecipitation from an asynchronous population of HeLa cells, with anti-APC7 antibodies. We subsequently isolated protein bands following SDS-PAGE and analyzed tryptic peptides using a Thermo Fisher Scientific LCQ DECA XP Plus ion trap as described previously (14). In addition to identifying peptides specific for APC7, a number of APC/C subunits and the APC/C E2, UbcH10, we also isolated peptides specific for TIF1 $\gamma$  (amino acid residues 394-407, KLLQQQNDITGLSR and 482-504, PAPGYTPNVVVVGQVPPGNTNHISK). To verify these findings we made an antibody that was specific for TIF1 $\gamma$  (Fig. 1A; Fig. 3A) and then assessed the ability of the APC/C holoenzyme to interact with TIF1 $\gamma$ . Reciprocal immunoprecipitation-Western blot analyses revealed that TIF1 $\gamma$  co-immunoprecipitated with a number of distinct APC/C subunits, and that APC/C components co-immunoprecipitated with TIF1 $\gamma$  (Fig. 1A and 1B). These analyses revealed that TIF1 $\gamma$  associated preferentially

with a higher molecular weight form of APC7, though it also bound the major APC7 form as well (Fig. 1B). Further analyses revealed that TIF1 $\gamma$  associated specifically with the APC/C activator Cdc20, but did not associate with Cdh1 (Fig. 1C; Fig 1D). To assess the stoichiometry of TIF1 $\gamma$  association with the APC/C we next determined the ability of TIF1 $\gamma$ , relative to APC/C activators, Cdc20 and Cdh1, to bind to APC/C subunits. This experiment revealed that TIF1 $\gamma$  associated with a smaller pool of APC3, relative to Cdc20 and Cdh1, and a smaller pool of APC5, relative to Cdc20 (Fig. 1D). These analyses also revealed that TIF1 $\gamma$  associated more efficiently with the higher molecular weight form of APC7 than Cdc20 or Cdh1, though TIF1 $\gamma$ , Cdc20 and Cdh1, all bound the major form of APC7 with equal avidity (Fig. 1D). GST pull-downs revealed that TIF1 $\gamma$  associated preferentially with APC3 and Cdc20 (Fig. 1E). As TIF1 $\gamma$  binds the APC/C, and possesses three potential RxxL destruction box motifs within its primary sequence (residues 440-443, 968-971 and 1114-1117) we next investigated whether TIF1 $\gamma$  is a target for APC/C ubiquitin ligase activity. First we performed *in vitro* ubiquitin ligase assays with anti-APC3 immunoprecipitates using [<sup>35</sup>S]-labelled TIF1 $\gamma$  or [<sup>35</sup>S]-labelled cyclin B1 as substrates. Consistent with previous findings cyclin B1 was efficiently polyubiquitylated in an APC/C-dependent manner, whereas TIF1 $\gamma$  was not a target for APC/C-directed ubiquitin ligase activity in this assay (Fig. 1F). Next, we assessed TIF1 $\gamma$  protein levels *in vivo*, following the release of cells from a nocodazole-induced mitotic block. In accordance with the *in vitro* APC/C ligase assays, cyclin B1 levels were reduced significantly following the passage of cells through mitosis and into the successive G1 phase, whilst levels of the TIF1 $\gamma$  protein were not altered following release of the cells from the mitotic block (Fig. 1G). It appeared however, that TIF1 $\gamma$  was subject to post-translational modification in nocodazole-treated cells, as gauged by reduced mobility upon SDS-PAGE (Fig. 1G). To corroborate our findings that TIF1 $\gamma$  is not targeted for degradation by the APC/C we next assessed TIF1 $\gamma$  protein levels following the exogenous expression of Myc-tagged Cdc20 and Cdh1 (Fig. 1H). TIF1 $\gamma$  levels remained unaffected following the expression of Cdc20 or Cdh1, whereas the levels of APC/C-Cdc20 substrate, NEK2A, were reduced following Myc-tagged Cdc20 expression, and levels of APC/C-Cdh1 substrate, PLK1, were reduced following the expression of Myc-tagged Cdh1 (Fig. 1H). In agreement with these findings TIF1 $\gamma$  protein levels were not altered following the ablation of Cdc20, or Cdh1, expression by RNAi (Fig. 3A). To substantiate these findings we next determined whether knockdown of the APC/C inhibitor, Emi1 (15, 16), or knockdown of Cdh1, affected TIF1 $\gamma$  protein levels following release from a mitotic block (Fig 1I). This experiment revealed that although Emi1 knockdown, relative to non-silencing controls, prevented the re-accumulation of cyclin A 18 hours after nocodazole release, it did not affect appreciably the levels of TIF1 $\gamma$  (*cf* lane 4 and lane 8; Fig 1I). Similarly, Cdh1 knockdown allowed for the precocious accumulation of cyclin B1 at 18 hours after nocodazole release, but did not enhance TIF1 $\gamma$  levels (*cf* lane 4 and lane 12; Fig. 1I). Taken together these data indicate that TIF1 $\gamma$  associates preferentially with APC/C-Cdc20, but that TIF1 $\gamma$  is not a substrate for APC/C-Cdc20-, or APC/C-Cdh1-, directed ubiquitylation.

### TIF1 $\gamma$ associates preferentially with the APC/C in mitosis and S phase

As Cdc20 binding to the APC/C is cell cycle-regulated and TIF1 $\gamma$  binds preferentially to APC/C-Cdc20, we thought it appropriate to examine the ability of TIF1 $\gamma$  to bind to the APC/C during each stage of the cell cycle. To do this we collected highly enriched populations of mitotic, G1, S and G2 HeLa cells and subjected them to immunoprecipitation with anti-APC7 antibodies, followed by Western blotting for TIF1 $\gamma$ . Consistent with the ability of TIF1 $\gamma$  to bind APC/C-Cdc20, we determined that TIF1 $\gamma$  had a greater capacity to bind the APC/C in mitosis than in G1 or G2 phases, despite TIF1 $\gamma$  levels not changing appreciably during the cell cycle (Fig. 2A). TIF1 $\gamma$  also had a greater ability to bind the APC/C in S-phase, relative to its ability to bind the APC/C in G1 and G2 phases (Fig. 2A). Cell cycle

status was verified by blotting for cell cycle-regulated proteins (Fig. 2A). Given that TIF1 $\gamma$  associates preferentially with Cdc20, and not Cdh1 (Fig. 1), and that TIF1 $\gamma$  interaction with the APC/C is cell cycle-dependent (Fig. 2A), we hypothesized that TIF1 $\gamma$  might associate with the APC/C only in discrete phases of mitosis. To investigate this possibility we immunoprecipitated APC7 complexes from nocodazole-treated cells, and those cells released back into the cell cycle following nocodazole withdrawal, and subsequently performed Western blots for TIF1 $\gamma$ . Interestingly, the ability of TIF1 $\gamma$  to bind the APC/C was maximal in SAC-activated cells, but was reduced appreciably once the SAC was satisfied and cells were allowed to progress through mitosis (Fig. 2B). To establish whether TIF1 $\gamma$  also bound Cdc20 in a cell cycle-dependent manner we next immunoprecipitated Cdc20 and TIF1 $\gamma$  from mitotic, G1, S and G2 populations of HeLa cells and performed the corresponding TIF1 $\gamma$  and Cdc20 Western blots (Fig. 2C). These analyses revealed that TIF1 $\gamma$  associated with Cdc20, exclusively in mitosis, suggesting a role for TIF1 $\gamma$ -APC/C-Cdc20 complexes, specifically in mitosis (Fig. 2C). Given these findings and those that suggest that TIF1 $\gamma$  associates with APC3 and Cdc20 independently (Fig. 1D), we next determined whether Cdc20, or Cdh1, knockdown affected the ability of TIF1 $\gamma$  to interact with the APC/C holoenzyme (Fig. 2D). Significantly, the ability of TIF1 $\gamma$  to associate with the APC/C was not affected by Cdc20, or Cdh1 knockdown, suggesting that TIF1 $\gamma$  might also affect APC/C function, independent of its association with Cdc20. These data suggest that TIF1 $\gamma$  associates directly with the APC/C. Whether TIF1 $\gamma$  associates with Cdc20 directly, *in vivo*, remains unknown.

### TIF1 $\gamma$ knockdown stabilizes the levels of APC/C substrates and blocks cells in mitosis

To address the functional significance of the TIF1 $\gamma$ -APC/C interaction we first investigated whether TIF1 $\gamma$  expression affects the levels of known APC/C substrates. We therefore ablated TIF1 $\gamma$  expression in HeLa cells using two different siRNAs and then determined the protein levels of different APC/C substrates by Western blotting. As positive controls we also determined the effects of Cdc20 and Cdh1 knockdown upon APC/C substrate levels. These analyses revealed that the knockdown of TIF1 $\gamma$ , Cdc20 and Cdh1 was highly efficient; knockdown was essentially complete after 24h and protein levels remained low for the duration of the experiment (Fig. 3A). Consistent with the notion that TIF1 $\gamma$  might regulate APC/C ligase activity, the protein levels of APC/C substrates cyclin A, cyclin B1, Aurora A, PLK1 and Cdc20 were all elevated in cells treated with siRNAs against TIF1 $\gamma$ , relative to non-silencing controls (Fig. 3A). Cdc20 and Cdh1 knockdown affected the protein levels of APC/C substrates as expected (Fig. 3A). Given these findings, we next investigated whether TIF1 $\gamma$  knockdown affected cell cycle distribution. We therefore treated asynchronous HeLa cells with the appropriate siRNAs and then determined cell cycle status 72h post treatment (Fig 3B). Propidium iodide staining indicated that there were a greater proportion of TIF1 $\gamma$  knockdown cells in G2/M, relative to non-silencing controls (Fig 3B). In accordance with the established role of the APC/C in mitosis and the affect of TIF1 $\gamma$  knockdown on the levels of APC/C substrates, phospho-serine 10 histone H3 staining revealed that there was also a dramatic increase in the mitotic index following TIF1 $\gamma$  knockdown, relative to non-silencing controls (Fig 3B). Treatment of cells with the TIF1 $\gamma$ -1i siRNA caused a greater than 14-fold increase in the mitotic index relative to non-silencing siRNA, whilst TIF1 $\gamma$ -2i siRNA increased the number of cells in mitosis approximately 6-fold (Fig. 3B). As TIF1 $\gamma$  also regulates transcription we next investigated whether TIF1 $\gamma$  knockdown affected the protein levels of APC/C subunits (Fig. 3C). Significantly, ablation of TIF1 $\gamma$  expression by RNAi did not down-regulate the protein levels of APC/C subunits (Fig. 3C), suggesting that TIF1 $\gamma$  transcriptional activity does not account for its affects upon the APC/C. Taken together, these data are important in establishing a potential role for TIF1 $\gamma$  in modulating APC/C activity and regulating cell cycle progression.

### TIF1 $\gamma$ knockdown prolongs time taken to progress through mitosis

Given these findings we next addressed whether TIF1 $\gamma$  regulates progression through mitosis. We therefore performed live-cell Differential Interference Contrast (DIC), and immunofluorescent, video microscopy with HeLa cells expressing EGFP-labelled  $\alpha$ -tubulin and mCherry-labelled histone H2B and calculated the time taken for cells, treated with non-silencing siRNA or siRNAs targeted against TIF1 $\gamma$ , to progress from the beginning of NEBD to anaphase (Fig. 4). Consistent with a role for TIF1 $\gamma$  in mitosis, cells treated with non-silencing siRNA took on average 105.2 min to pass from NEBD to anaphase, whilst cells treated with siRNAs targeted against TIF1 $\gamma$ , TIF1 $\gamma$ -1i and TIF1 $\gamma$ -2i, took 199.04 min and 142.2 min, respectively (cf Fig 4A-C). Interestingly, a large proportion of the cells treated with siRNAs targeted against TIF1 $\gamma$  appeared to have prolonged metaphases that were characterized by a failure to undergo metaphase-to-anaphase transition (Fig. 4E). Indeed, image analysis revealed that those TIF1 $\gamma$  knockdown cells that failed to undergo metaphase-to-anaphase transition were characterized at late times by plasma membrane blebbing, compacted chromatin and aberrant mitotic spindle formation. Close inspection of the data revealed that only three cells of fifty analyzed took over 300 min to pass from NEBD to anaphase following treatment with non-silencing siRNA (Fig. 4A), whilst there was a 3-fold increase in the number of cells taking over 300 min to pass from NEBD to anaphase following treatment with TIF1 $\gamma$  siRNAs (Fig. 4). Taken together these data are supportive of the notion that TIF1 $\gamma$  functions to regulate progression through mitosis.

### TIF1 $\gamma$ knockdown leads to an accumulation of cells in metaphase

To substantiate these findings further we next investigated whether TIF1 $\gamma$  knockdown affects mitotic distribution. To do this we treated asynchronous HeLa cells with either non-silencing siRNAs or siRNAs targeted against TIF1 $\gamma$  and determined the number of cells in prophase, prometaphase, metaphase, anaphase and telophase by immunofluorescent microscopy. Consistent with the observation that TIF1 $\gamma$  knockdown affects progression from NEBD to anaphase, it was notable that TIF1 $\gamma$  knockdown with either TIF1 $\gamma$  siRNA caused a significant increase in the number of metaphase cells and a corresponding, significant decrease in the number of anaphase and telophase cells (Fig. 5A). These data are supportive of the idea that TIF1 $\gamma$  regulates metaphase-to anaphase transition.

### Loss of TIF1 $\gamma$ expression results in SAC activation

It was evident whilst analyzing the effect of TIF1 $\gamma$  knockdown upon mitotic distribution that although all TIF1 $\gamma$  knockdown cells in metaphase had a characteristic bipolar spindle, the majority of these cells (>90%) had misaligned chromosomes. We reasoned therefore that TIF1 $\gamma$  depletion might result in the activation of the SAC. To address this possibility, we treated HeLa cells with either non-silencing siRNAs or siRNAs targeted against TIF1 $\gamma$  and assessed Bub1 association with kinetochores. Consistent with the idea that the SAC is activated following TIF1 $\gamma$  knockdown, microscopic studies revealed that Bub1 was associated with the kinetochores of misaligned chromosomes at metaphase in TIF1 $\gamma$  knockdown cells (Fig. 5B). Furthermore, Western blotting revealed that TIF1 $\gamma$  knockdown promoted the upregulation, and phosphorylation, of SAC regulators Bub1 and BubR1 (Fig. 5C). To substantiate these findings we next attempted to override the SAC phenotype displayed by TIF1 $\gamma$  knockdown cells, by coordinately ablating the expression of both TIF1 $\gamma$  and BubR1 (Fig. 5D). Consistent with the hypothesis that TIF1 $\gamma$  knockdown activates the SAC, we determined that cells depleted of TIF1 $\gamma$  alone had elevated levels of cyclin B1, phospho-serine 10 histone H3 and phosphorylated BubR1 (Fig. 5D), whilst cells depleted of both TIF1 $\gamma$  and BubR1 had substantially reduced levels of cyclin B1 and phospho-serine 10 histone H3, relative to cells treated with non-silencing siRNA or TIF1 $\gamma$  siRNA (Fig. 5D). These results indicate that knockdown of BubR1 relieves SAC activation induced by TIF1 $\gamma$



knockdown, and allows for metaphase-to anaphase transition and mitotic exit. Taken together these data indicate that the SAC is activated following TIF1 $\gamma$  knockdown, and that TIF1 $\gamma$  regulates APC/C function prior to anaphase.

### TIF1 $\gamma$ is also associated with the APC/C-MCC in SAC-activated cells

To examine the relationship between TIF1 $\gamma$  and the SAC in more detail we investigated the ability of TIF1 $\gamma$  to associate with BubR1, the APC/C and Cdc20 upon SAC activation. Initially, we determined the relative abilities of TIF1 $\gamma$  and the APC/C to associate with Cdc20 and BubR1 in asynchronously growing HeLa cells, and HeLa cells collected by mitotic shake-off where the SAC was activated by nocodazole treatment (Fig. 5E). In line with our studies examining TIF1 $\gamma$  association with the APC/C, both the APC/C and TIF1 $\gamma$  had a greater propensity to bind to Cdc20 and BubR1 in mitosis following SAC activation (Fig. 5E). Consistent with these findings, the APC/C also had a greater propensity to bind BubR1 when TIF1 $\gamma$  levels were depleted by siRNA (Fig. 5E). There was however, only a modest increase in TIF1 $\gamma$ -APC7 association following SAC activation, suggesting that TIF1 $\gamma$  association with the APC/C holoenzyme is largely SAC-independent (Fig. 5E). As APC15 has recently been implicated in controlling the SAC by regulating the APC/C-dependent turnover of MCC components (17) we investigated whether TIF1 $\gamma$  was also involved in regulating MCC turnover. To do this we activated the SAC in HeLa cells and monitored MCC attachment to the APC/C in cells where TIF1 $\gamma$  or APC15 had been depleted by siRNA. Consistent with its known function, APC15 depletion stabilized MCC association with the APC/C, whilst TIF1 $\gamma$  did not (Fig. 5F). These data indicate that although TIF1 $\gamma$  is associated with the APC/C-MCC in SAC-activated cells it is not required to inactivate the SAC.

### Role for TIF1 $\gamma$ in APC/C-mediated degradation of cyclin A and cyclin B1 in mitosis

To determine a direct role for TIF1 $\gamma$  in the APC/C-mediated degradation of APC/C substrates in mitosis, we next performed *in vitro* APC/C ubiquitin ligase assays upon anti-APC3 immunoprecipitates from HeLa cells treated with either non-silencing siRNA, or siRNA against TIF1 $\gamma$ . These experiments revealed that TIF1 $\gamma$  knockdown, relative to non-silencing controls, reduced substantially the ability of the APC/C to polyubiquitylate [<sup>35</sup>S]-labelled cyclin A by about 80% (Fig. 6A). As cyclin A degradation is typically SAC-independent (18, 19), these data are supportive of a model whereby TIF1 $\gamma$  modulates APC/C-Cdc20 activity directly to regulate the polyubiquitylation of cyclin A. To determine whether the impairment of APC/C ubiquitin ligase activity in TIF1 $\gamma$  knockdown cells also extends to SAC-dependent substrates, we assessed the ability of the APC/C immunoprecipitated from HeLa cells, treated with either non-silencing siRNA, or siRNA against TIF1 $\gamma$ , to ubiquitylate cyclin B1 (Fig. 6A). Consistent with a more general role for TIF1 $\gamma$  in the regulation of APC/C activity, TIF1 $\gamma$  knockdown, relative to non-silencing controls, reduced the ability of the APC/C to polyubiquitylate [<sup>35</sup>S]-labelled cyclin B1 by approximately 60% (Fig. 6A).

Since the APC/C and Cdc20 cooperate in binding substrates (20, 21), and data presented here has determined that TIF1 $\gamma$  associates with APC/C-Cdc20, and affects APC/C-Cdc20 activity in mitosis, we next investigated whether TIF1 $\gamma$  was also able to associate with the APC/C substrates, cyclin A and cyclin B1. Consistent with the idea that TIF1 $\gamma$  modulates APC/C activity during mitosis, TIF1 $\gamma$  was able to bind cyclin A *in vivo* (Fig. 6B); it was not however, able to bind cyclin B1 (Fig. 6B). Consistent with this finding [<sup>35</sup>S]-labelled TIF1 $\gamma$  also associated specifically with GST-cyclin A *in vitro* (Fig. 6B). Taken together these data support the notion that TIF1 $\gamma$  promotes the APC/C-Cdc20-dependent degradation of cyclin A in mitosis potentially through interaction with the APC/C holoenzyme, Cdc20, and cyclin A itself. These data also suggest that TIF1 $\gamma$  can affect APC/C E3 ligase activity directed

towards cyclin B1, independently of binding to cyclin B1. As the APC/C-mediated degradation of cyclin A normally begins at the onset of NEBD in mitosis (22), we next investigated whether cyclin A expression was elevated in metaphase cells where TIF1 $\gamma$  expression had been ablated by RNAi. As before, TIF1 $\gamma$  knockdown resulted in metaphase cells with misaligned chromosomes (Fig 6C). Consistent with the Western blot data (Fig. 3A), confocal microscopy revealed that cyclin A levels were higher in TIF1 $\gamma$  knockdown cells at metaphase, relative to cells treated with non-silencing siRNA (Fig 6C); TIF1 $\gamma$  cells expressing elevated levels of cyclin A at metaphase had characteristic misaligned chromosomes (Fig 6C).

### TIF1 $\gamma$ mitotic effects are dependent upon the SAC

As overexpression of exogenous cyclin A has previously been reported to result in chromosome misalignment and anaphase delay in a SAC-independent manner (22), we wanted to discern whether TIF1 $\gamma$  knockdown affected cell cycle progression through mitosis independently of the SAC through the modulation of endogenous cyclin A levels, or, alternatively affected mitotic progression in a SAC-dependent manner. To do this, we investigated by DIC, and immunofluorescent, video microscopy the effect of dual TIF1 $\gamma$  and BubR1 knockdown in HeLa cells upon the time taken for cells to progress from NEBD to anaphase (Fig. 7). As we previously demonstrated, TIF1 $\gamma$  knockdown alone resulted in a significant delay in the ability of cells to progress through mitosis and undergo metaphase-to-anaphase transition (Figs. *cf* 7A and 7B; Fig. 7F), whereas BubR1 knockdown alone resulted in more rapid progress from NEBD to anaphase, relative to control cells, presumably as the SAC had been inactivated (*cf* Figs. 7A and 7C). Cells that were depleted of both TIF1 $\gamma$  and BubR1 progressed through mitosis with similar kinetics to those cells that had been treated with BubR1 siRNA alone (*cf* Fig. 7C and 7D). Taken together these data suggest that the ability of TIF1 $\gamma$  to affect cell cycle progression through mitosis is mediated exclusively through the SAC.

### Cellular expression of a siRNA-resistant TIF1 $\gamma$ facilitates mitotic progression and mitotic exit

As TIF1 $\gamma$  knockdown leads to the accumulation of APC/C substrates and SAC activation, we reasoned that expression of a siRNA-resistant TIF1 $\gamma$  might restore APC/C activity against mitotic substrates and allow cells to progress through, and exit mitosis. To investigate this possibility we first ablated TIF1 $\gamma$  expression by siRNA and, 48h later, transfected knockdown cells with a siRNA-resistant FLAG-tagged TIF1 $\gamma$  species. We harvested cells 24h post-transfection and performed Western blot analyses to determine the consequences of TIF1 $\gamma$  expression on APC/C function (Fig. 7G). Importantly, these analyses revealed that expression of the siRNA-resistant FLAG-tagged TIF1 $\gamma$  species reversed TIF1 $\gamma$  knockdown effects, and led to a significant reduction in the levels of the APC/C substrate, cyclin A, and the mitotic indicator, phospho-serine 10 histone H3 (Fig. 7G). Taken together these data support the notion that TIF1 $\gamma$  regulates APC/C activity directly and allows for the temporally coordinated, APC/C-dependent progression of cells through mitosis.

## DISCUSSION

In this report we have identified TIF1 $\gamma$  as an APC3 and Cdc20 binding protein that associates specifically *in vivo* with the APC/C holoenzyme, APC/C-Cdc20 and APC/C-MCC complexes and promotes mitotic progression (Fig. 1-7). In this regard TIF1 $\gamma$  associated with a number of APC/C subunits *in vivo* (Fig. 1). Interestingly, TIF1 $\gamma$  associated with two forms of APC7, a major 66 kDa species, and a minor 75 kDa species; TIF1 $\gamma$  associated preferentially with the minor species (Figs. 1B and 1D). It is not clear at present whether this minor species of APC7 represents an APC7 isoform, or whether it is a post-

translationally modified form of the major APC7 species. It will be important to characterize the minor form of APC7 as it might give new insight into APC/C function. We also presented considerable evidence to indicate that TIF1 $\gamma$  is not a substrate for APC/C-dependent ubiquitylation (Fig. 1; Fig 3C), and that it associated preferentially with Cdc20 and not Cdh1 (Fig.1). Perhaps surprisingly, TIF1 $\gamma$  associated with the APC/C in S phase as well G2 and mitosis (Fig. 2). Previous reports have suggested that Emi1 acts as a pseudosubstrate inhibitor of the APC/C to prevent premature APC/C activation (15, 16); it will be of interest to determine whether TIF1 $\gamma$  functions in a similar manner to regulate APC/C activity during S phase. Our data also revealed that TIF1 $\gamma$  associated with Cdc20 preferentially in mitosis (Fig. 2), and that Cdc20 knockdown did not appreciably affect TIF1 $\gamma$  association with the APC/C (Fig. 2). It will be of interest in the future therefore, to dissect the relative contributions of TIF1 $\gamma$ -APC/C- and TIF1 $\gamma$ -Cdc20 interactions in controlling mitotic progression.

It is now well established that APC/C-Cdc20 promotes the degradation of early mitotic substrates such as Nek2A and cyclin A (22, 23) and initiates metaphase-to-anaphase transition by promoting the polyubiquitylation and proteasomal-mediated degradation of the Separase inhibitor, Securin (1, 2). We determined that TIF1 $\gamma$  knockdown reduces APC/C ligase activity, stabilizes APC/C substrates and increases the number of cells in metaphase, relative to control-treated cells (Figs. 3, 5 and 6). Our studies also revealed that TIF1 $\gamma$  knockdown prolonged the time taken for cells to pass from NEBD to anaphase, and that a significant proportion of TIF1 $\gamma$  knockdown cells failed to undergo metaphase-to-anaphase transition (Figs. 4 and 5A). Consistent with these findings, we established that TIF1 $\gamma$  knockdown promotes SAC activation (Fig. 5). The notion that TIF1 $\gamma$  inactivation promotes SAC activation is supported by the observation that knockdown of the SAC component, BubR1, can overcome SAC activation imposed by TIF1 $\gamma$  knockdown (Fig. 5D; Fig 7). However, unlike APC15 which regulates SAC by coordinating MCC dissociation from the APC/C, TIF1 $\gamma$  does not play a role in regulating SAC inactivation (Fig. 5F). A direct role for TIF1 $\gamma$  in mitotic progression was given credence by the observation that siRNA-resistant TIF1 $\gamma$  relieves SAC activation, promotes cyclin A degradation, and facilitates cell cycle progression through mitosis (Fig. 7G). Collectively, these data indicate that, not only does TIF1 $\gamma$  modulate APC/C-Cdc20 activity and the progression of cells through mitosis, it also associates with the APC/C-MCC.

The APC/C-Cdc20-mediated degradation of early mitotic substrates such as cyclin A occurs despite SAC activation (19, 24). It has been suggested that cyclin A outcompetes SAC proteins for binding to Cdc20, and that cyclin A-Cdc20 complexes are subsequently recruited to the APC/C by the cyclin-dependent kinase cofactor, Cks (19, 24). As TIF1 $\gamma$  binds specifically to APC/C-Cdc20 complexes and cyclin A *in vivo*, and has the capability to bind to Cdc20, APC3 and cyclin A independently *in vitro* (Fig. 1; Fig. 6B), it is possible that TIF1 $\gamma$  cooperates with Cdc20 and Cks in the binding and recruitment of cyclin A to the APC/C. Given that TIF1 $\gamma$  knockdown also affects the ability of the APC/C to polyubiquitylate cyclin A (Fig. 6A), TIF1 $\gamma$  might facilitate the degradation of cyclin A by modulating APC/C-Cdc20 ligase activity directly. The notion that TIF1 $\gamma$  functions directly to regulate APC/C activity is supported by the observations that the APC/C-Cdc20-dependent degradation of cyclin A is SAC-independent, and that significantly more APC/C ligase activity against cyclin A can be immunoprecipitated from asynchronous cells relative to TIF1 $\gamma$  knockdown cells, even though there are between 5- and 10-fold more cells in mitosis following TIF1 $\gamma$  knockdown (*cf* Fig. 5A and Fig. 6A). A more general role for TIF1 $\gamma$  in modulating APC/C ubiquitin ligase activity is given credence by the observation that TIF1 $\gamma$  knockdown also affects the ability of the APC/C to polyubiquitylate cyclin B1 (Fig. 6A). It is possible therefore that TIF1 $\gamma$  might function more generally to affect APC/C ligase activity directed towards its substrates.



Pertinently, it has previously been demonstrated that cyclin A is targeted for degradation by APC/C-Cdc20 at the commencement of NEBD, and that cyclin A degradation is required for proper chromosome alignment at metaphase; cyclin A overexpression delays chromosome alignment and anaphase onset (22). As TIF1 $\gamma$  knockdown leads to an increase in metaphase cells, a concomitant reduction in the number of anaphase and telophase cells, and the stabilization of cyclin A at metaphase (Fig. 3; Fig. 6B), it could be reasoned that increased cyclin A expression in TIF1 $\gamma$  knockdown cells is responsible, at least in part, for the mitotic phenotype observed in these cells (Fig. 3; Fig. 4). It has been suggested that cyclin A overexpression delays metaphase-to-anaphase transition independently of SAC as MAD2 does not appear to associate with kinetochores in this instance, though whether it promotes BubR1 association with the APC/C, akin to TIF1 $\gamma$  knockdown, has not been investigated (22). As SAC inactivation relieves completely the mitotic phenotype imposed by TIF1 $\gamma$  knockdown (Fig. 5D; Fig. 7), our data indicates that SAC inactivation overcomes any cell cycle restrictions imposed by the inappropriate presence of endogenous cyclin A at metaphase in TIF1 $\gamma$  knockdown cells, such that chromosome misalignment at metaphase in TIF1 $\gamma$  knockdown cells is subject to control by the SAC (Fig. 7). It is perhaps not surprising that the TIF1 $\gamma$  knockdown phenotype shares only some characteristics of the cyclin A overexpression phenotype, as it might be expected that TIF1 $\gamma$  knockdown reduces APC/C ligase activity directed against other substrates that modulate progression through mitosis (Fig 3A; Fig. 6A). In this regard, it is possible that the reduction of APC/C activity *per se* in TIF1 $\gamma$  knockdown cells, leads to the accumulation of APC/C substrates that activate and/or sustain the SAC. It is also possible that TIF1 $\gamma$  has other activities in mitosis, unrelated to its ability to affect APC/C ligase activity that regulates chromosome attachment. For instance, TIF1 $\gamma$  might ubiquitylate components of the kinetochore or MCC to coordinate chromosome attachment. TIF1 $\gamma$  association with chromatin might also promote mitotic progression. These possibilities however, await investigation.

Indeed, it has recently been reported that the cell permeable, prodrug form of the small molecule inhibitor of the APC/C, tosyl-L-arginine methyl ester (TAME), proTAME, induces a SAC-dependent metaphase arrest in the absence of spindle damage (25). As the proteasome inhibitor, MG132 also promotes a SAC-dependent mitotic arrest, the authors of this article proposed that APC/C-dependent proteolysis was required to inactivate the SAC, and that APC/C inhibition activated the SAC. Interestingly, some laboratories have proposed that the APC/C-mediated ubiquitylation, but not degradation, of Cdc20 releases the APC/C from SAC inhibition (26, 27), though we and others suggest that APC/C-mediated ubiquitylation and degradation of Cdc20 sustains the SAC (28, 29). As pro-TAME activates the SAC in an APC/C-dependent manner, without chromosome misalignment at metaphase, it could be reasoned that the reduction in APC/C ligase activity in TIF1 $\gamma$  knockdown cells similarly activates the SAC through the stabilization of multiple APC/C substrates. In accordance with this hypothesis, Cdc20, cyclin B1, Aurora A and PLK1 are all elevated in TIF1 $\gamma$  knockdown cells (Fig. 3A). As cyclin-dependent kinase activity has previously been shown to sustain the SAC (30, 31), it is possible that elevated cyclin expression, and presumably therefore, cyclin-dependent kinase activity in TIF1 $\gamma$  knockdown cells also sustains activation of the SAC and prevents metaphase-to-anaphase transition. Alternatively, other APC/C substrates elevated in TIF1 $\gamma$  knockdown cells might similarly promote chromosome misalignment and activate and/or sustain the SAC by targeting SAC components through post-translational modification or protein-protein interaction. Indeed, Bub1 and BubR1 are both APC/C substrates (32, 33) and are activated and elevated following TIF1 $\gamma$  knockdown (Figs. 5B and 5C). Pertinent to this idea, transgenic overexpression of Bub1 in mice gives rise to metaphases with misaligned chromosomes, aneuploidy and tumour formation (34) whilst expression of an acetylated BubR1 mimetic mutant inhibits the APC/C-mediated degradation of BubR1 and leads to a delay in anaphase onset (33).

Consistent with our observations that TIF1 $\gamma$  modulates APC/C-Cdc20 activity, TIF1 $\gamma$  binds to the APC/C preferentially in mitosis and S-phase, and binds to Cdc20 exclusively in mitosis (Fig. 2). Interestingly TIF1 $\gamma$  binding to the APC/C was unaffected by Cdc20 knockdown, suggesting that TIF1 $\gamma$  binds proportionally to more APC/C holoenzyme than Cdc20 (Fig. 2D). Further analyses revealed that TIF1 $\gamma$  is associated with the APC/C-MCC in SAC-activated cells, but loses the ability to bind the APC/C once the SAC had been satisfied (Fig. 2B). This observation suggests that TIF1 $\gamma$  might participate actively in SAC inactivation by promoting the APC/C-mediated degradation of substrates prior to anaphase that maintain SAC activation. Taken together the data presented herein suggests that TIF1 $\gamma$  associates with the APC/C holoenzyme, active APC/C-Cdc20 complexes, and the APC/C-MCC, and as such participates in the regulation of APC/C-Cdc20 complexes during mitosis.

It has been reported that the TGF- $\beta$  antagonist, SnoN is a critical target for APC/C-Cdh1-mediated degradation in TGF- $\beta$ -stimulated cells (35, 36). As we have determined that TIF1 $\gamma$  associates specifically with the Cdc20-bound form of the APC/C, and not the Cdh1-bound form (Fig. 1), these data suggest that TIF1 $\gamma$  does not promote the APC/C-dependent degradation of SnoN in TGF- $\beta$ -stimulated cells. However, as APC/C-Cdc20 has recently been implicated in regulating presynaptic axonal differentiation programmes (37) it is possible that TIF1 $\gamma$ -APC/C-Cdc20 complexes could participate in TGF- $\beta$  signaling pathways that coordinate cell cycle exit and cellular differentiation (38).

In conclusion data presented here demonstrates a role for TIF1 $\gamma$  in regulating APC/C function in mitosis. We propose that TIF1 $\gamma$  associates specifically with the APC/C in order to promote the temporally-coordinated destruction of APC/C substrates and progression of cells through mitosis.

## MATERIALS AND METHODS

### Antibodies

The anti-Cdc20, APC1, APC4, APC6, APC8, cyclin A, cyclin B1, PLK1 anti-Myc and phospho-Histone H3 (serine-10) antibodies were from Santa Cruz. The anti-Cdh1 antibody was from Neomarkers, the anti- $\beta$ -actin, anti- $\alpha$ -tubulin and vinculin antibodies were from Sigma, the anti-histone H3 antibody was from Millipore, the anti-Bub1 and anti-Aurora A antibodies were from Abcam, the anti-Bub3, anti-BubR1 and NEK2 antibodies were from Becton Dickinson, the anti-APC15 antibody was from Sigma, and the anti-APC3 antibodies were from Becton Dickinson or CR-UK. Anti-APC5, APC4, APC7 and APC11 antibodies have been described previously (4, 29). The rabbit polyclonal against TIF1 $\gamma$  was raised against an N-terminal protein fragment (residues 1-392). Anti-mouse and anti-rabbit HRP antibodies were from Dako. Alexa - 488 and -555 fluorophores were from Invitrogen.

### Plasmids

APC/C subunits, UbcH4, UbcH5, UbcH10, Cdc20, cyclin A and TIF1 $\gamma$  were cloned into pGEX4T-1 for bacterial expression. pcDNA3-cyclin A and pcDNA3-cyclin B1 were used for *in vitro* transcription/translation. pCS2-FLAG-TIF1 $\gamma$  construct was used for *in vitro* and mammalian expression. Myc-tagged Cdc20 and Cdh1 constructs were from addgene.

### Cells and treatments

HeLa cells were maintained in Dulbecco's modified Eagle's medium (Sigma) supplemented with 8% foetal calf serum and 2 mM L-glutamine (Invitrogen) and cultured at 37°C in humidified incubators supplied with 5% CO<sub>2</sub>. Cells were arrested in prometaphase by treatment with 200ng/ml nocodazole for 20 hours and collected by shake off. G1 cells were collected 3 hours after nocodazole release, and remaining mitotic cells were removed by

shake-off. Cells were synchronized at the G1-S border by double thymidine block (2.5mM). G2 cells were obtained by release from double thymidine block for 8 hours followed by mitotic shake-off (39, 40).

### Immunoprecipitation and GST pull-down

Cells were lysed using immunoprecipitation buffer (50 mM Tris-HCl, pH 7.4, 0.825 M NaCl, 1% (v/v) NP-40) and clarified by sonication and centrifugation. Immunoprecipitation was then performed as described previously (41). L- $\alpha$ -[<sup>35</sup>S]-methionine-labelled TIF1 $\gamma$  was expressed *in vitro* using a TNT T7 Coupled Reticulocyte Lysate System (Promega) according to the manufacturer's guidelines. *In vitro* glutathione-S-transferase (GST) pulldown assays using GST, GST-APC/C and GST-Cdc20 proteins were then performed using established protocols (42).

### SDS-PAGE and Western blotting

Whole-cell protein extracts were prepared in denaturing buffer (9 M urea, 150 mM  $\beta$ -mercaptoethanol, 50 mM Tris-HCl, pH 7.4). Extracts were clarified by sonication, and protein concentrations determined by Bradford assay (Bio-Rad). Proteins were separated by SDS-PAGE in the presence of 100 mM Tris, 100 mM Bicine and 0.1% (w/v) SDS. Proteins were then transferred onto nitrocellulose membranes (Pall), before being blocked in Tris-buffered saline containing 5% (w/v) dried milk powder and 0.1% (v/v) Tween 80 and incubation with the appropriate antibodies. Antigens were visualized by enhanced chemiluminescence.

### RNA interference and transfections

The sequences of the siRNA oligonucleotides, purchased from Ambion, were CCUGCAUCUAGAAAGUGAAAdTdT (TIF1 $\gamma$ -1i), GCGACUGAUUACUUCCAGdTdT (TIF1 $\gamma$ -2i), GGAAAUAGCCGAGAGGUAAdTdT (APC3), GUCUGGUCUAAGUUUCUUdTdT (APC15) and CGUACGCGGAAUACUUCGAdTdT (control). The BubR1 siRNA used was a Dharmacon on target plus SMARTpool. SiRNAs were transfected using Oligofectamine (Invitrogen) as described previously (41). HeLa cells were transfected with a siRNA resistant FLAG-tagged TIF1 $\gamma$  expression construct using Lipofectamine 2000 (Invitrogen). FLAG-TIF1 $\gamma$  was rendered insensitive to TIF1 $\gamma$ -1i siRNA by the introduction of two silent mutations: CCUGCAUCUGGAGAGUGAAAdTdT

### Mass spectrometry

Immunoprecipitates isolated on Protein G Sepharose beads were separated by SDS-PAGE and stained with Coomassie Brilliant Blue (Sigma). Protein bands were excised and subject to treatment with 10 mM DTT and then 50 mM iodoacetamide. Bands were dried then subject to treatment with trypsin (Promega). Tryptic peptides were analyzed by positive electrospray ionisation/mass spectrometry, using a Thermo Fisher Scientific LCQ DECA XP Plus ion trap as described previously (14). Mass spectrometry/mass spectrometry raw data were searched against a non-redundant human protein database using TurboSEQUENT, as part of the BioworksBrowser 3.1 software suite.

### Video microscopy

Live cell imaging was performed using a Deltavision core microscope (Applied precision) equipped with an incubation chamber maintained at 37°C in an atmosphere of 5% CO<sub>2</sub>. Videos were acquired at seven-minute intervals using a magnification objective of 40 and Softworx software.

### APC/C ligase assays

APC/C complexes were immunoprecipitated from cells using anti-APC3 mAb and protein G sepharose. APC/C ubiquitin ligase activity was assayed as described (4) and resolved by SDS-PAGE. Gels were then dried and visualized by autoradiography.

### Confocal microscopy

Cells were seeded onto poly-L-lysine-coated glass slides and fixed and permeabilized with methanol cooled to  $-20^{\circ}\text{C}$ . Slides were then incubated for 1 h at room temperature in blocking buffer (2 % (v/v) foetal calf serum in PBS), and then incubated for 2 h with the primary antibody diluted in blocking buffer. Slides were then washed in PBS, and incubated for 2 h with secondary antibody diluted in blocking buffer. After further washing in PBS, slides were mounted in Vectashield containing DAPI (Vectorlabs). Cells were observed and images were acquired using a Zeiss LSM510-Meta laser scanning confocal microscope.

### FACS analysis

Cells were fixed in 70% (v/v) ethanol for 1 h, and then washed with PBS prior to permeabilisation in PBS containing 0.25 % (v/v) Triton X-100. After washing with 1 % (w/v) BSA in PBS, cells were incubated with an anti-phosphohistone H3 (Ser10) polyclonal antibody in 1 % (w/v) BSA in PBS for 1.5 h at room temperature. Samples were then washed twice with 1% (w/v) BSA in PBS, and incubated for 1 h with a fluorescein isothiocyanate (FITC)-conjugated-anti-Rabbit antibody diluted in 1 % w/v BSA in PBS. After washing with PBS alone, cells were resuspended in PBS containing propidium iodide (25  $\mu\text{g}/\text{ml}$ ) and 0.1 mg/ml of RNase A, and left at room temperature for a further 1 h. Cell cycle analysis was then carried out using a Coulter XL-MCL flow cytometer (Beckman-Coulter).

### Acknowledgments

We would like to thank Francis Barr, Andrew Fry, Stefano Piccolo, Frank Rauscher III, Hughes de Thé and Hiroyuki Yamano for reagents. This work was funded by CR-UK (C10000/A7542) and The University of Birmingham, College of Medical and Dental Sciences Research Development Fund. JN is supported by The Danish Cancer Society and the Lundbeck Foundation.

### REFERENCES

1. Peters JM. The anaphase promoting complex/cyclosome: a machine designed to destroy. *Nat Rev Mol Cell Biol.* 2006; 7:644–656. [PubMed: 16896351]
2. Musacchio A, Salmon ED. The spindle-assembly checkpoint in space and time. *Nat Rev Mol Cell Biol.* 2007; 8:379–393. [PubMed: 17426725]
3. Yu H. Cdc20: A WD40 Activator for a Cell Cycle Degradation Machine. *Mol. Cell.* 2007; 27:3–16. [PubMed: 17612486]
4. Turnell AS, Stewart GS, Grand RJ, Rookes SM, Martin A, Yamano H, et al. The APC/C and CBP/p300 cooperate to regulate transcription and cell-cycle progression. *Nature.* 2005; 438:690–695. [PubMed: 16319895]
5. Turnell AS, Mymryk JS. Roles for the coactivators CBP and p300 and the APC/C E3 ubiquitin ligase in E1A-dependent cell transformation. *Br. J. Cancer.* 2006; 95:555–560. [PubMed: 16880778]
6. Townsend K, Mason H, Blackford AN, Miller ES, Chapman JR, Sedgwick GG, et al. Mediator of DNA damage checkpoint 1 regulates mitotic progression. *J. Biol. Chem.* 2009; 284:33939–33948. [PubMed: 19826003]
7. Venturini L, You J, Stadler M, Galien R, Lallemand V, Koken MH, et al. TIF1gamma, a novel member of the transcriptional intermediary factor 1 family. *Oncogene.* 1999; 18:1209–1217. [PubMed: 10022127]

8. Peng H, Feldman I, Rauscher FJ 3rd. Hetero-oligomerization among the TIF family of RBCC/TRIM domain-containing nuclear cofactors: a potential mechanism for regulating the switch between coactivation and corepression. *J. Mol. Biol.* 2002; 320:629–644. [PubMed: 12096914]
9. Klugbauer S, Rabes HM. The transcription coactivator HTIF1 and a related protein are fused to the RET receptor tyrosine kinase in childhood papillary thyroid carcinomas. *Oncogene.* 1999; 18:4388–4393. [PubMed: 10439047]
10. Ransom DG, Bahary N, Niss K, Traver D, Burns C, Trede NS, et al. The zebrafish moonshine gene encodes transcriptional intermediary factor 1 gamma, an essential regulator of hematopoiesis. *PLoS Biol.* 2004; 2:E237, 1188–1196. [PubMed: 15314655]
11. He W, Dorn DC, Erdjument-Bromage H, Tempst P, Moore MA, Massague J. Hematopoiesis controlled by distinct TIF1gamma and Smad4 branches of the TGFbeta pathway. *Cell.* 2006; 125:929–941. [PubMed: 16751102]
12. Dupont S, Zacchigna L, Cordenonsi M, Soligo S, Adorno M, Rugge M, et al. Germ-layer specification and control of cell growth by Ectodermin, a Smad4 ubiquitin ligase. *Cell.* 2005; 121:87–99. [PubMed: 15820681]
13. Dupont S, Mamidi A, Cordenonsi M, Montagner M, Zacchigna L, Adorno M, et al. FAM/USP9x, a deubiquitinating enzyme essential for TGFbeta signaling, controls Smad4 monoubiquitination. *Cell.* 2009; 136:123–135. [PubMed: 19135894]
14. Shimwell NJ, Martin A, Bruton RK, Blackford AN, Gallimore PH, Turnell AS, et al. Adenovirus 5 early region 1A associates with insulin receptor substrates. *Oncogene.* 2009; 28:686–697. [PubMed: 19029952]
15. Reimann JD, Freed E, Hsu JY, Kramer ER, Peters JM, Jackson PK. Emi1 is a mitotic regulator that interacts with Cdc20 and inhibits the anaphase promoting complex. *Cell.* 2001; 105:645–655. [PubMed: 11389834]
16. Miller JJ, Summers MK, Hansen DV, Nachury MV, Lehman NL, Loktev A, Jackson PK. Emi1 stably binds and inhibits the anaphase-promoting complex/cyclosome as a pseudosubstrate inhibitor. *Genes Dev.* 2006; 20:2410–20. [PubMed: 16921029]
17. Mansfeld J, Collin P, Collins MO, Choudhary JS, Pines J. APC15 drives the turnover of MCC-CDC20 to make the spindle assembly checkpoint responsive to kinetochore attachment. *Nat. Cell Biol.* 2011; 13:1234–1243. [PubMed: 21926987]
18. Hunt T, Luca FC, Ruderman JV. The requirements for protein synthesis and degradation, and the control of destruction of cyclins A and B in the meiotic and mitotic cell cycles of the clam embryo. *J. Cell Biol.* 1992; 116:707–724. [PubMed: 1530948]
19. Di Fiore B, Pines J. How cyclin A destruction escapes the spindle assembly checkpoint. *J. Cell Biol.* 2010; 190:501–509. [PubMed: 20733051]
20. Matsykiela ME, Morgan DO. Analysis of activator-binding sites on the APC/C supports a cooperative substrate-binding mechanism. *Mol. Cell.* 2009; 34:68–80. [PubMed: 19362536]
21. Izawa D, Pines J. How APC/C-Cdc20 changes its substrate specificity in mitosis. *Nat. Cell Biol.* 2011; 13:223–233. [PubMed: 21336306]
22. den Elzen N, Pines J. Cyclin A is destroyed in prometaphase and can delay chromosome alignment and anaphase. *J. Cell Biol.* 2001; 153:121–136. [PubMed: 11285279]
23. Hayes MJ, Kimata Y, Wattam SL, Lindon C, Mao G, Yamano H, et al. Early mitotic degradation of Nek2A depends on Cdc20-independent interaction with the APC/C. *Nat. Cell Biol.* 2006; 8:607–614. [PubMed: 16648845]
24. Wolthuis R, Clay-Farrace L, van Zon W, Yekezare M, Koop L, Ogink J, et al. Cdc20 and Cks direct the spindle checkpoint-independent destruction of cyclin A. *Mol. Cell.* 2008; 30:290–302. [PubMed: 18471975]
25. Zeng X, Sigoiilot F, Gaur S, Choi S, Pfaff KL, Oh DC, et al. Pharmacologic inhibition of the anaphase-promoting complex induces a spindle checkpoint-dependent mitotic arrest in the absence of spindle damage. *Cancer Cell.* 2010; 18:382–395. [PubMed: 20951947]
26. Reddy SK, Rape M, Margansky WA, Kirschner MW. Ubiquitination by the anaphase promoting complex drives spindle checkpoint inactivation. *Nature.* 2007; 446:921–925. [PubMed: 17443186]



27. Stegmeier F, Rape M, Draviam VM, Nalepa G, Sowa ME, Ang XL, et al. Anaphase initiation is regulated by antagonistic ubiquitination and deubiquitination activities. *Nature*. 2007; 446:876–881. [PubMed: 17443180]
28. Ge S, Skaar JR, Pagano M. APC/C- and Mad2-mediated degradation of Cdc20 during spindle checkpoint activation. *Cell Cycle*. 2009; 8:167–171. [PubMed: 19098431]
29. Nilsson J, Yekezare M, Minshull J, Pines J. The APC/C maintains the spindle assembly checkpoint by targeting Cdc20 for destruction. *Nat. Cell Biol.* 2008; 10:1411–1420. [PubMed: 18997788]
30. Chung E, Chen RH. Phosphorylation of Cdc20 is required for its inhibition by the spindle checkpoint. *Nat Cell Biol.* 2003; 5:748–753. [PubMed: 12855955]
31. D'Angiolella V, Mari C, Nocera D, Rametti L, Grieco D. The spindle checkpoint requires cyclin-dependent kinase activity. *Genes Dev.* 2003; 17:2520–2525. [PubMed: 14561775]
32. Qi W, Yu H. KEN-box-dependent degradation of the Bub1 spindle checkpoint kinase by the anaphase-promoting complex/cyclosome. *J. Biol. Chem.* 2007; 282:3672–3679. [PubMed: 17158872]
33. Choi E, Choe H, Min J, Choi JY, Kim J, Lee H. BubR1 acetylation at prometaphase is required for modulating APC/C activity and timing of mitosis. *EMBO J.* 2009; 28:2077–2089. [PubMed: 19407811]
34. Ricke RM, Jeganathan KB, van Deursen JM. Bub1 overexpression induces aneuploidy and tumor formation through Aurora B kinase hyperactivation. *J. Cell Biol.* 2011; 193:1049–1064. [PubMed: 21646403]
35. Wan Y, Liu X, Kirschner MW. The anaphase-promoting complex mediates TGF- $\beta$  signaling by targeting SnoN for destruction. *Mol. Cell.* 2001; 8:1027–1039. [PubMed: 11741538]
36. Zhang L, Fujita T, Wu G, Xiao X, Wan Y. Phosphorylation of APC/Cdc27 is involved in TGF- $\beta$  signaling. *J. Biol. Chem.* 2011; 286:10041–10050. [PubMed: 21209074]
37. Yang Y, Kim AH, Yamada T, Wu B, Bilimoria PM, Ikeuchi Y, et al. A Cdc20-APC ubiquitin signaling pathway regulates presynaptic differentiation. *Science*. 2009; 326:575–578. [PubMed: 19900895]
38. Massagué J, Gomis RR. The logic of TGF $\beta$  signaling. *FEBS Lett.* 2006; 580:2811–2820. [PubMed: 16678165]
39. Chaudhry MA, Chodosh LA, McKenna WG, Muschel RJ. Gene expression profiling of HeLa cells in G1 or G2 phases. *Oncogene*. 2002; 21:1934–1942. [PubMed: 11896627]
40. Xu YX, Manley JL. New insights into mitotic chromosome condensation: a role for the prolyl isomerase Pin1. *Cell Cycle*. 2007; 23:2896–2901. [PubMed: 17993783]
41. Blackford AN, Patel RN, Forrester NA, Theil K, Groitl P, Stewart GS, et al. Adenovirus E4orf6 inhibits ATR activation by promoting TOPBP1 degradation. *Proc. Natl. Acad. Sci. U S A.* 2010; 107:12251–12256. [PubMed: 20566845]
42. Rasti M, Grand RJA, Yousef YF, Shuen M, Mymryk JS, Gallimore PH, et al. Roles for APIS and the 20S proteasome in adenovirus E1A-dependent transcription. *EMBO J.* 2006; 25:2710–2722. [PubMed: 16763564]

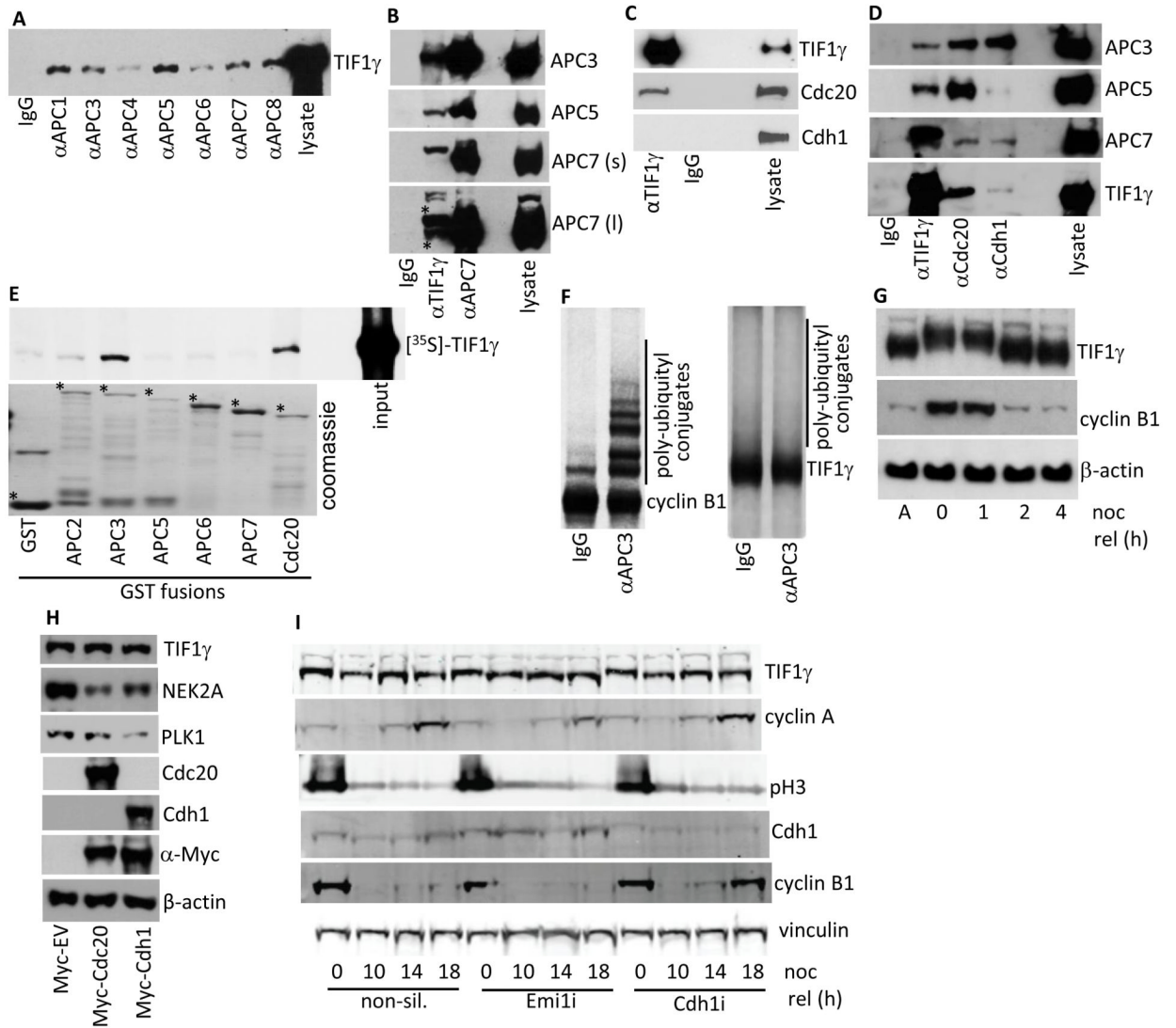


**Figure 1. TIF1 $\gamma$  associates with the APC/C but is not a substrate for APC/C ligase activity**  
**(A-D)** APC/C components, Cdc20, Cdh1 and TIF1 $\gamma$  were immunoprecipitated from asynchronous whole cell HeLa extracts, separated by SDS-PAGE, and Western blotted for coprecipitating proteins. APC7 (s), short exposure; APC7 (l), long exposure. **(E)** TIF1 $\gamma$  binds to APC3 and Cdc20 *in vitro*. GST and GST-APC2, APC3, APC5, APC6, APC7 and Cdc20 fusion proteins were incubated with L- $\alpha$ -[ $^{35}$ S]-methionine labeled TIF1 $\gamma$  GST-fusion, and binding proteins were purified upon glutathione-agarose beads and separated by SDS-PAGE. The binding of TIF1 $\gamma$  to GST proteins was assessed following autoradiography of the dried gel. \*indicates full-length GST fusion protein; upper band in GST lane is GST dimer **(F)** APC/C complexes were immunoprecipitated from asynchronous whole cell HeLa extracts using an anti-APC3 monoclonal antibody. APC/C immune complexes were assayed for E3 ligase activity in the presence of L- $\alpha$ -[ $^{35}$ S]-methionine labeled cyclin B1 or TIF1 $\gamma$ . After 1 h incubation samples were separated by SDS-PAGE. Polyubiquitylation of cyclin B1 and TIF1 $\gamma$  was assessed following autoradiography of the dried gel. **(G)** TIF1 $\gamma$  is post-translationally modified in response to nocodazole treatment but it is not degraded following nocodazole release (noc rel). HeLa cells were treated with 200ng/ml nocodazole for 20h. Mitotic cells were then isolated by shake-off and either harvested, or released back into

cycle following the removal of nocodazole and then harvested at later times. Proteins were separated by SDS-PAGE and then Western blotted for TIF1 $\gamma$ , cyclin B1 and  $\beta$ -actin. Lane 1: asynchronous cells (A); lane 2: mitotic shake-off following nocodazole treatment (0); lanes 3-5: 1, 2 and 4h post nocodazole release. **(H)** TIF1 $\gamma$  is not targeted for degradation by Cdc20 or Cdh1. HeLa cells were transfected with mammalian expression plasmids expressing either Myc-tag alone (Myc-EV), Myc-tagged Cdc20, or Myc-tagged Cdh1. Samples were harvested 24h post-transfection and subject to SDS-PAGE and Western blotting. **(I)** Emi1 knockdown does not promote TIF1 $\gamma$  degradation. HeLa cells were treated with non-silencing siRNA, Emi1, and Cdh1 siRNAs. Forty-Eight h post-knockdown cells were treated with 200 ng/ml nocodazole for 20h. Mitotic shake-off cells were then released from the nocodazole block (noc rel) and harvested at the times indicated and subject to SDS-PAGE and Western blotting.

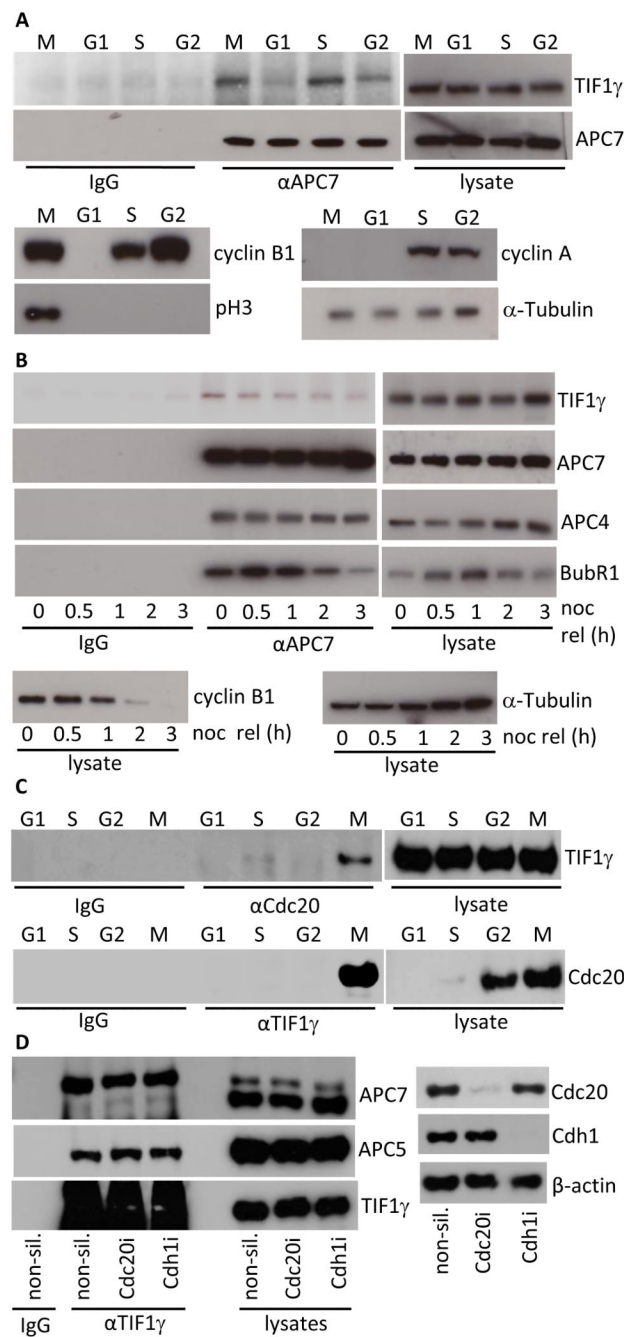


**Figure 2. TIF1 $\gamma$  association with the APC/C and Cdc20 is cell-cycle dependent.**

(A) TIF1 $\gamma$  binds the APC/C preferentially in mitosis and S phase. HeLa whole cell extracts were prepared from G1, S, G2 and M phase enriched cell populations. APC7 was then immunoprecipitated from each fraction, isolated upon Protein G Sepharose, and the relative amount of TIF1 $\gamma$  associated with APC7 immune complexes was determined by Western blot. Cell cycle status was verified by Western blotting for cyclins A, B, phospho Ser10-Histone H3 (pH3) and  $\alpha$ -tubulin. (B) The ability of TIF1 $\gamma$  to bind the APC/C decreases once the SAC is satisfied and cells progress through mitosis. HeLa cells were treated with 200ng/ml nocodazole for 20h. Mitotic cells were then isolated by shake-off and either harvested, or

released back into cycle following the removal of nocodazole and then harvested at later times. APC7 was then immunoprecipitated from cell lysates, isolated upon Protein G Sepharose and TIF1 $\gamma$  binding to the APC/C was assessed by Western blot. Levels of BubR1, cyclin B1, APC4, APC7, TIF1 $\gamma$  and  $\alpha$ -tubulin were also assessed by Western blot. **(C)** TIF1 $\gamma$  binds Cdc20 preferentially in mitosis. HeLa whole cell extracts were prepared from G1, S, G2 and M phase enriched cell populations. Cdc20 and TIF1 $\gamma$  was then immunoprecipitated from each fraction, isolated upon Protein G Sepharose, and the relative amount of TIF1 $\gamma$  associated with Cdc20 was determined by Western blot. **(D)** Cdc20 knockdown does not affect APC/C association with TIF1 $\gamma$  HeLa cells were treated with non-silencing siRNA, Cdc20, and Cdh1 siRNAs. Forty-Eight h post-knockdown cells were harvested and subject to immunoprecipitation with anti-TIF1 $\gamma$  antibodies Following SDS-PAGE TIF1 $\gamma$  association with the APC/C was assessed by Western blotting.



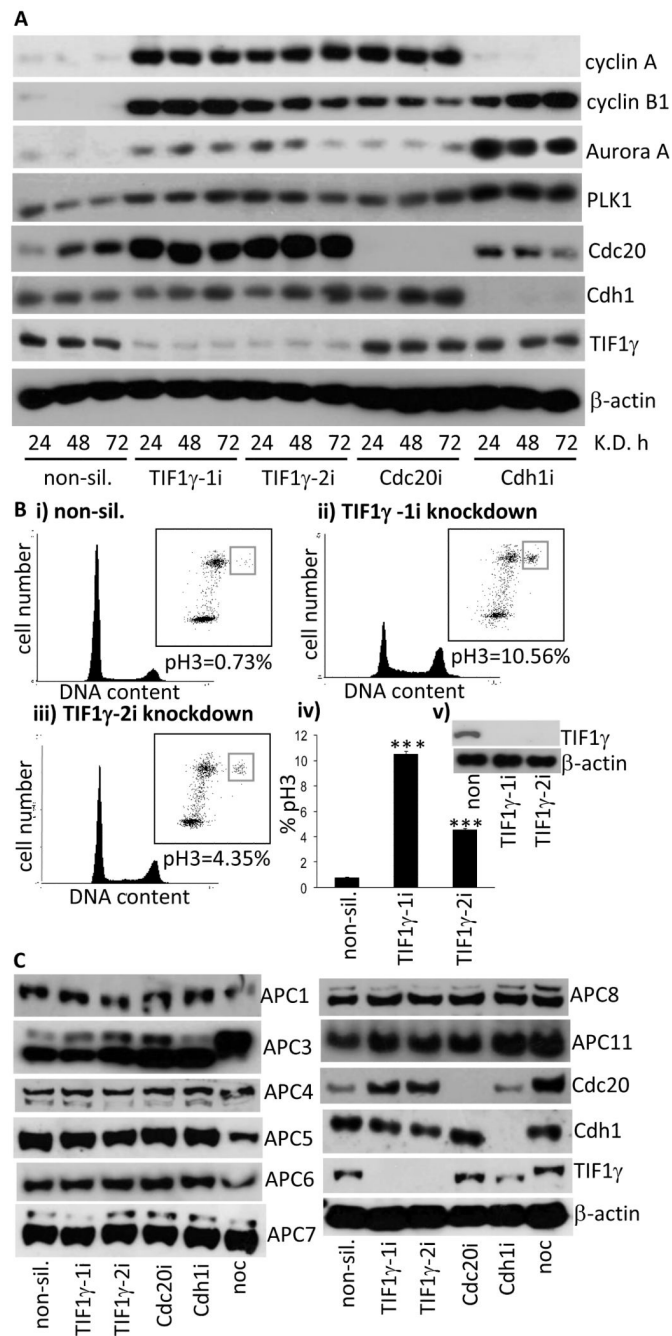


**Figure 3. Ablation of TIF1 $\gamma$  expression by RNA interference stabilizes APC/C substrates and increases the number of cells in mitosis**

(A) Mitotic APC/C substrates are stabilized following TIF1 $\gamma$  knockdown. HeLa cells were treated with either non-silencing siRNA, or siRNAs specific for TIF1 $\gamma$ . Cell lysates were prepared at the times indicated and levels of APC/C substrates determined by Western blotting. TIF1 $\gamma$  levels were determined to monitor knockdown efficiency and  $\alpha$ -actin levels were determined as a loading control. (B) TIF1 $\gamma$  knockdown increases the mitotic index. HeLa cells were treated with either non-silencing siRNA, or siRNAs specific for TIF1 $\gamma$ . Cells were fixed in 70% (v/v) ice-cold ethanol 72h post-transfection and subsequently subjected to FACS analysis, following co-staining with propidium iodide, to gauge cell

cycle distribution, and an anti-phospho Ser10-Histone H3 antibody to gauge the numbers of cells specifically in mitosis. \*\*\* $P < 0.001$ ; data taken from three independent experiments. Error bars represent standard deviation. (C) TIF1 $\gamma$  knockdown does not affect APC/C subunit expression. HeLa cells were treated with either non-silencing siRNA, or siRNAs specific for TIF1 $\gamma$ , Cdc20 and Cdh1. Forty-Eight h post-knockdown cells were harvested and subject to SDS-PAGE and Western blotting.

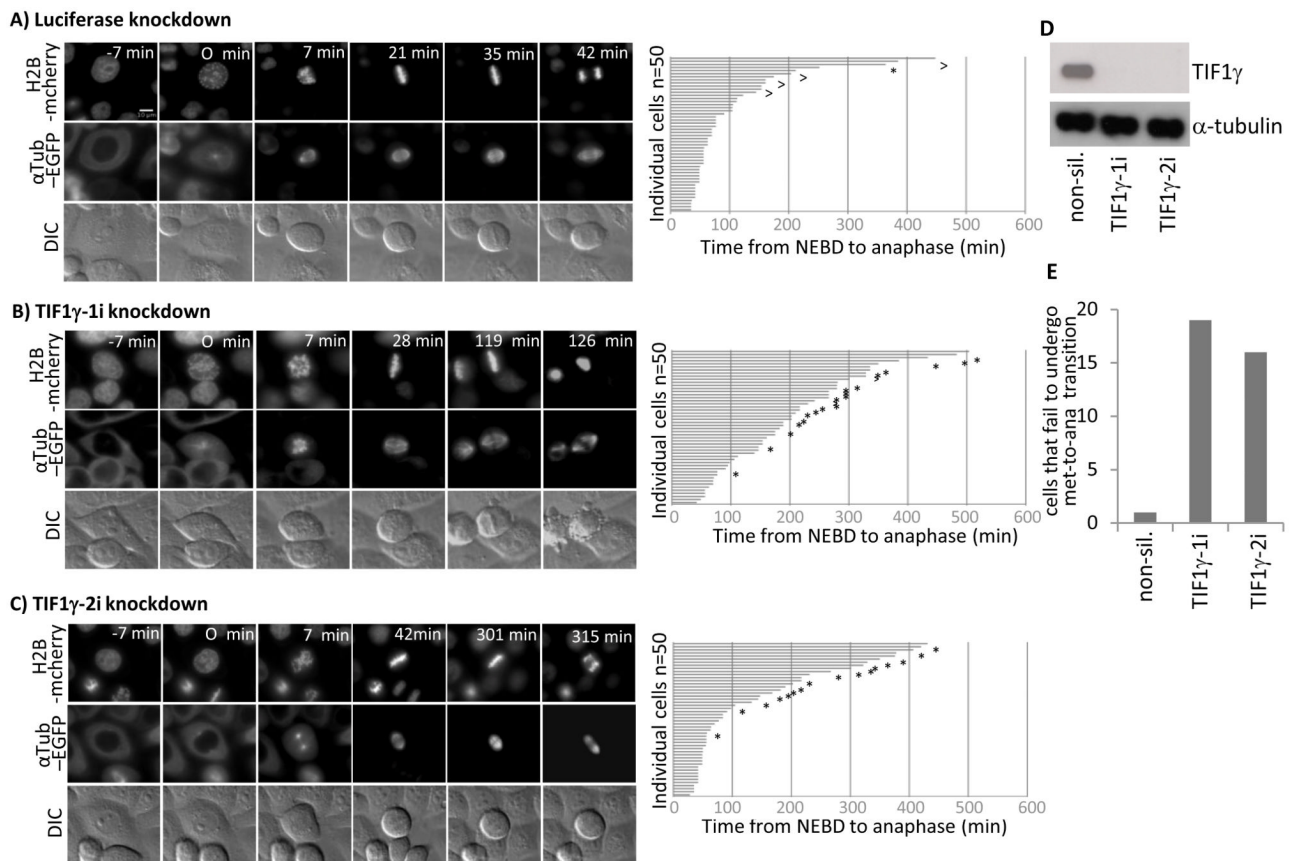


**Figure 4. TIF1 $\gamma$  knockdown delays progression through mitosis from NEBD to anaphase**  
 HeLa cells expressing Histone H2B mCherry and  $\alpha$ -tubulin-EGFP were treated with either an siRNA specific for luciferase or siRNAs specific for TIF1 $\gamma$  48h post-knockdown cells were subjected to a thymidine block for 16 h, whereupon cells were released back into cycle and video imaging began 9 h later. Video images representative of treatments with (A) luciferase siRNA (B) TIF1 $\gamma$ -1i siRNA and (C) TIF1 $\gamma$ -2i siRNA are presented. Corresponding bar charts illustrating the time taken for cells to progress from NEBD to anaphase are also presented. ^ represents cells that failed to exit mitosis during filming. \* represents cells that failed to undergo successful metaphase-to-anaphase transition during filming (depicted in Fig. 4E). DIC and immunofluorescent imaging revealed that those cells that failed to undergo metaphase-to-anaphase transition were characterized at late times by plasma membrane blebbing, compacted chromatin and aberrant mitotic spindle formation. Video imaging was therefore terminated at this time, and the time taken from NEBD to this point was recorded. The mean values calculated for time taken from NEBD to anaphase are therefore, underestimated for those cells that failed to undergo metaphase-to-anaphase transition. (D) Western blot for TIF1 $\gamma$  and  $\alpha$ -tubulin in cells treated with luciferase siRNA, TIF1 $\gamma$ -1i or TIF1 $\gamma$ -2i siRNAs.

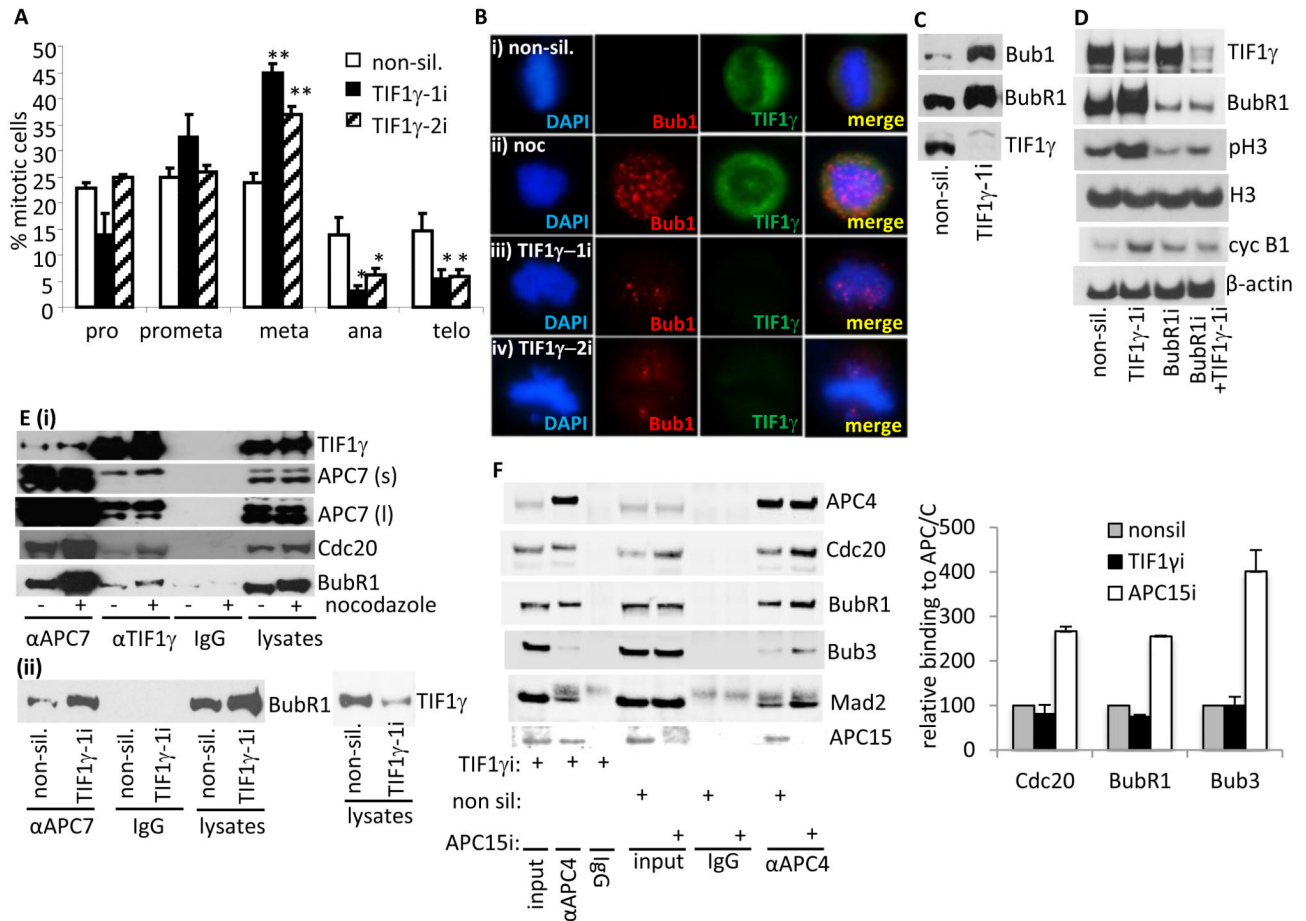


**Figure 5. Ablation of TIF1 $\gamma$  expression by RNA interference delays progression through mitosis and activates the SAC**

(A and B) TIF1 $\gamma$  knockdown increases the number of cells with misaligned chromosomes at metaphase. HeLa cells were treated with either non-silencing siRNA or siRNAs specific for TIF1 $\gamma$  and seeded onto glass slides. 72h post-transfection cells were fixed and permeabilized and then co-stained with either  $\alpha$ -tubulin, TIF1 $\gamma$  and DAPI, TIF1 $\gamma$  and DAPI, or Bub1, TIF1 $\gamma$  and DAPI, to gauge mitotic index, mitotic distribution and SAC activation. Nocodazole-treated cells were included as a control. (A) pro, prophase; prometa, prometaphase; meta, metaphase; ana, anaphase; telo, telophase. TIF1 $\gamma$  knockdown cells exhibiting a bipolar spindle and misaligned chromosomes at metaphase, were scored as metaphase cells. The bar chart represents results from three independent experiments (At least 300 mitotic cells were counted per experiment). Error bars denote standard deviation. \*P<0.05; \*\*P<0.01. (B) Immunofluorescent visualization of Bub1 associated with unattached kinetochores and attached kinetochores not under full tension in TIF1 $\gamma$  knockdown cells (276 out of 300 TIF1 $\gamma$ -1 metaphase knockdown cells had misaligned chromosomes and positive Bub1 staining whilst 253 out of 300 TIF1 $\gamma$ -2 metaphase knockdown cells had misaligned chromosomes and positive Bub1 staining compared to 17 out of 300 for non-silencing controls). (C) TIF1 $\gamma$  knockdown activates the SAC. HeLa cells were treated with either non-silencing siRNA, or siRNAs specific to TIF1 $\gamma$ . The levels of TIF1 $\gamma$  and the SAC proteins, BubR1 and Bub1 were determined by Western blotting 72h post knockdown. (D) BubR1 knockdown relieves SAC activation imposed by TIF1 $\gamma$  knockdown. HeLa cells were treated with either non-silencing siRNA, or siRNAs specific for TIF1 $\gamma$  BubR1, or TIF1 $\gamma$  and BubR1. Cell lysates were harvested after 72h and levels

of TIF1 $\gamma$ , BubR1, phospho Ser10-histone H3 (pH3), histone H3 (H3), cyclin B1 and  $\beta$ -actin were all determined by Western blotting. **(Ei)** TIF1 $\gamma$  associates with the APC/C-MCC in SAC-activated cells. HeLa cells were treated with nocodazole (200 ng/ml) for 20h. Cell lysates were then prepared and APC7 and TIF1 $\gamma$  were immunoprecipitated. The relative amounts of TIF1 $\gamma$ , APC7, Cdc20 and BubR1 associated with APC7 and TIF1 $\gamma$  were determined by Western blot. APC7 (s), short exposure; APC7 (l), long exposure. **(Eii)** HeLa cells were treated with either non-silencing siRNA, or siRNAs specific for TIF1 $\gamma$  APC7 and TIF1 $\gamma$  were immunoprecipitated from cell lysates prepared 72h post-transfection. The relative amount of BubR1 associated with APC7 was determined by Western blot. **(F)** HeLa cells were treated with either non-silencing siRNA, or siRNAs specific for TIF1 $\gamma$  or APC15 and 48h later, treated with nocodazole (200 ng/ml) for 20h. The association of Cdc20, BubR1 and Bub3 with the APC/C was assessed by Western blot following immunoprecipitation with an anti-APC4 antibody.



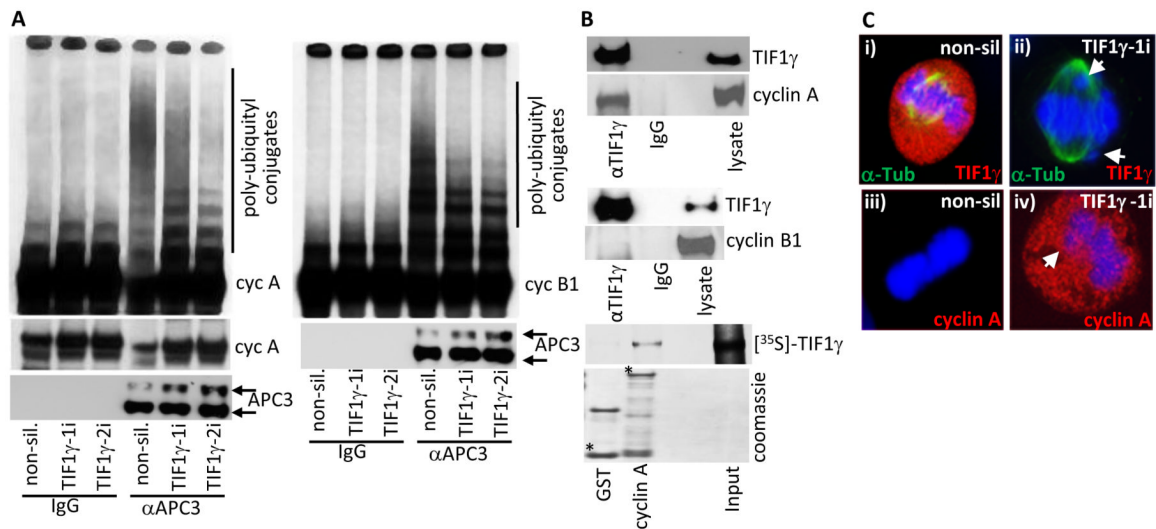


**Figure 6. Cyclin A is stabilized in mitotic TIF1 $\gamma$  knockdown cells and is degraded upon expression of an siRNA resistant TIF1 $\gamma$  species**

(A) APC/C ligase activity directed towards cyclin A and cyclin B1 is reduced following TIF1 $\gamma$  knockdown. HeLa cells were treated with either non-silencing siRNA, or siRNAs specific for TIF1 $\gamma$ . The APC/C holoenzyme was immunoprecipitated from cell lysates 72h post-treatment using an antibody to APC3. APC/C activity was then assayed by incubating anti-APC3 immunoprecipitates with L- $\alpha$ -[<sup>35</sup>S]-methionine labeled cyclin A or cyclin B1. After 1 h incubation samples were separated by SDS-PAGE and polyubiquitylation of cyclin A and cyclin B1 was assessed following autoradiography of the dried gel. (B) TIF1 $\gamma$  associates with cyclin A but not cyclin B1. HeLa cells were subject to immunoprecipitation with TIF1 $\gamma$ , and Western blotted for cyclin A or cyclin B1; GST and GST-cyclin A were incubated with L- $\alpha$ -[<sup>35</sup>S]-methionine labelled TIF1 $\gamma$  GST- fusion, and binding proteins were purified upon glutathione-agarose beads and separated by SDS-PAGE. The binding of TIF1 $\gamma$  to GST-cyclin A was assessed following autoradiography of the dried gel. \* indicates full-length GST fusion protein; upper band in GST lane is GST dimer. (C) Cyclin A is inappropriately present at metaphase in TIF1 $\gamma$  knockdown cells. HeLa cells were treated with either non-silencing siRNA or siRNAs specific for TIF1 $\gamma$  and seeded onto glass slides. 72h post-transfection cells were fixed and permeabilized and then co-stained with either  $\alpha$ -tubulin, TIF1 $\gamma$  and DAPI (i) or cyclin A and DAPI (ii)

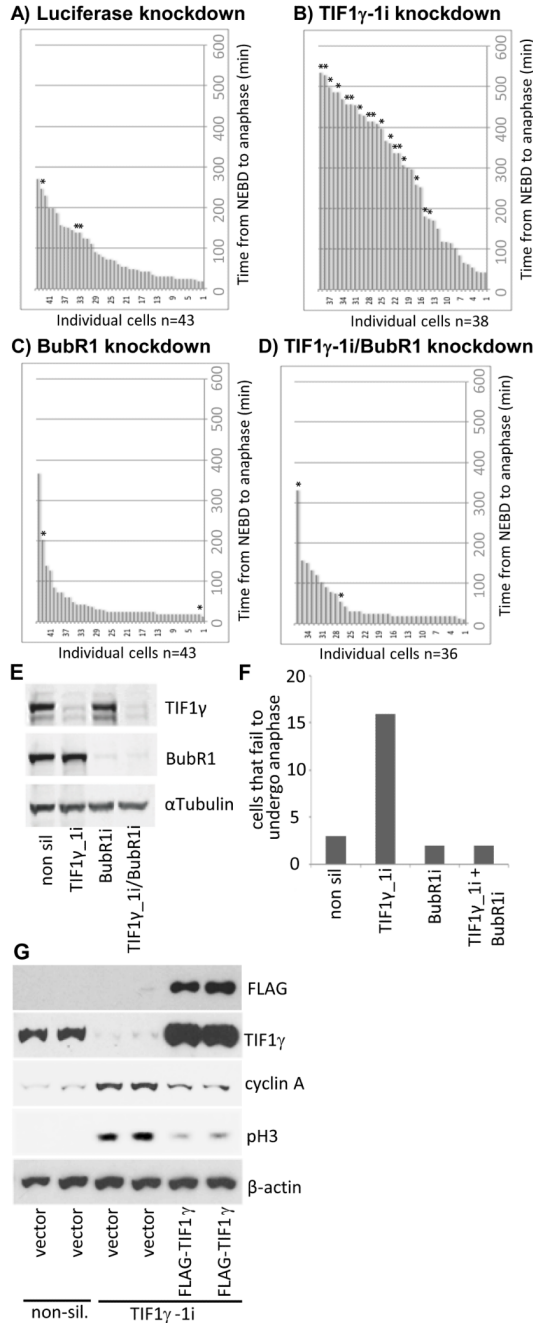


**Figure 7. Inactivation of the SAC allows TIF1 $\gamma$  knockdown cells to pass through mitosis from NEBD to anaphase**

HeLa cells expressing Histone H2B mCherry and  $\alpha$ -tubulin-EGFP were treated with either an siRNA specific for luciferase (A) or siRNAs specific for TIF1 $\gamma$  (B), BubR1 (C) or TIF1 $\gamma$  and BubR1 (D). 48h post-knockdown cells were subjected to a thymidine block for 16 h, whereupon cells were released back into cycle and video imaging began 9 h later. Bar charts depicting time taken to pass from NEBD to anaphase are presented. \* represents cells that failed to undergo successful metaphase-to-anaphase transition during filming (depicted graphically in Fig. 7F). (E) Western blots for TIF1 $\gamma$  BubR1 and  $\alpha$ -tubulin in cells treated with luciferase, TIF1 $\gamma$  BubR1, or  $\gamma$  and BubR1 siRNAs. (G) Expression of a siRNA-

resistant TIF1 $\gamma$  species allows for cyclin A degradation and mitotic progression. HeLa cells were treated with either non-silencing siRNA, or siRNAs specific for TIF1 $\gamma$  for 48 h. Cells were then transfected with vector alone or a construct expressing FLAG-TIF1 $\gamma$  and cultured for a further 24h. Cell lysates were prepared, and the levels of FLAG-TIF1 $\gamma$ , endogenous TIF1 $\gamma$ , cyclin A, phospho Ser10-histone H3 (pH3) and  $\beta$ -actin were all determined by Western blot.